Characteristic Analysis of DC and AC Fractional Order $RL_{\beta}C_{\alpha}$ Circuits for Stability Control and Performance Optimization

Zhengmao Ye[1][0000-0001-8897-574X], Hang Yin[1][0000-0002-4600-5881], Wanjun Wang[2][0000-0001-5605-8218], Shuju Bai[1][0000-0002-2463-0328], Habib Mohamadian[1][0000-0002-2099-2292], Fang Sun[3][0000-0002-0813-2046], Adrian Qing Meng[4][0000-0001-5419-710X], Yongmao Ye[5][0000-0002-0925-4678]

[1] College of Science and Engineering, Southern University, Baton Rouge, LA 70813, USA
zhengmao_ye@subr.edu, hang_yin@subr.edu, shuju_bai@subr.edu, habib_mohamadian@subr.edu
[2] College of Engineering, Louisiana State University, Baton Rouge, LA 70803, USA
wang@lsu.edu
[3] China Quality Certification Center, Beijing, 100070, China
sunfang@cqc.com.cn
[4] Huayang Canada, Toronto, ON L4B 1T4, Canada
adrian.meng@outlook.com
[5] Broadcasting Department, Liaoning Radio and Television Station, Shenyang, 110000, China
yeyongmao@hotmail.com

Abstract. Fractional order calculus has traditionally been applied to the chaotic theory and fractal analysis, which has also been gradually expanded to various engineering fields such as mechatronics, dynamic control and secure communication. Fractional order models provide extra degrees of freedom and flexible parameterization. The idea could be directly imposed on the fundamental RLC circuit design. The fractional differential equation will be formulated for both series and parallel fractional order $RL_{\beta}C_{\alpha}$ circuits. The behaviors of the DC fractional order $RL_{\beta}C_{\alpha}$ circuits can be examined through the step responses for stability analysis. I-V characteristics at the resonant frequency are critical in analysis of AC fractional order RLC circuits, which has numerous applications such as fractional-order filters and electromagnetics. Numerical simulations of the fractional order $RL_{\beta}C_{\alpha}$ systems have been conducted. Various performance comparisons are made to solve potential parametric optimization problems among diverse combinations of the fractional orders α and β.

Keywords: fractional order calculus, fractional $RL_{\beta}C_{\alpha}$ circuit, resonance, step response, stability control, dynamic stability

1 Introduction

Being a typical engineering application of the fractional order calculus, the fractional order $RL_{\beta}C_{\alpha}$ circuit can be modeled as a fractional differential equation to compare its characteristics with classical 2nd order RLC circuits. It is widely known in science for a long time that chaotic behaviors can be generated from fractional order differential equations, but applications of fractional order calculus to engineering problems are relatively new which have been extended to system identification, control, mechatronics, electromagnetics, robotics and communication so far. Controlling dynamic stability is a challenging issue in various engineering applications. One typical example is the automotive idle speed control problem, for which almost all existing control methodologies have been applied to ensure idle speed stability during the nonlinear transient process. It is promising to apply fractional order calculus to these complex engineering applications [1-2]. For instance, the fractional order itself has impact on the global stability of chaotic dynamical systems, such as the Lorenz dynamical system and Chua dynamical system, where synchronization and fractional order control could be applied [3]. Some interesting engineering problems are also solved via fractional order calculus. Integrated implementation of the parallel resonator covering a fractional-order capacitor and a fractional-order inductor has been proposed. It uses current-controlled transconductance operational amplifiers as building blocks, which is fabricated in AMS 0.35μm CMOS process. The electronic tuning capability is optimized based on the second-order approximation of fractional-order differentiator and integrator in the range of 10-700 Hz [4]. Fractional order PID (Proportional Integral Derivative) control has been used for the DC motor reference speed tracking with robustness against random disturbances. The optimal state estimation can be also achieved via integration with Kalman filter design [5]. All 2nd order circuits (e.g. 2nd order RLC, 2nd order notch filters) can be easily modeled via the transfer function and state space approaches for further analysis. It is feasible to offer additional degrees of freedom using fractional order circuits, but more complex mathematical models should be built in a similar way for better control [6-7]. The wireless power transmission calls for the high switching frequency to transmit energy effectively, however high-frequency switching and high efficiency are both challenging to existing switching devices. Fractional-order reactive elements in wireless power transmission are able to implement necessary functions at the lower switching frequency. It results in better high-frequency switching performance and higher efficiency. A generalized fractional order wireless power transmission is thus formulated together with comprehensive analysis. Results indicate that higher power efficiency and less switching frequency than classical methods can be reached [8].

In fields of electronics, practical implementation in terms of fractional order capacitors and fractional order inductors are possible. Fractional-order capacitor and inductor emulators have been presented based on current feedback operational amplifiers. Fractional order differentiator and integrator topologies are combined and implemented via the integer-order multiple feedback filter topology. Options on time constants and gain factors provide flexibility to the topology design between the fractional-order capacitor and inductor.

The emulator behavior has been successfully analyzed using the PSpice simulator [9]. Some basic analyses of fractional order circuits are also done where comparisons are made. A fractional differential equation for the electrical RLC circuit with limited fractional order $0<\gamma\leqslant 1$ is formulated. The auxiliary parameter γ characterizes the existence of fractional system components. Analytical solutions are given by the Mittag-Leffler function depending on the fractional order [10]. Time domain analysis of the fractional order model for the $RL_\beta C_\alpha$ circuits has been proposed to determine responses to arbitrary voltage inputs. An arbitrary non-integer fractional order can be represented as an infinite series of the Mittag-Leffler functions via Laplace transform. It leads to detailed description of complex electrical properties [11].

In addition, three different types of electrical circuit equations based on fractional calculus and several definitions of fractional derivatives are studied so that different types of solutions are compared with the classical solution [12]. For the fractional order $RL_\beta C_\alpha$ circuit with AC power supply, fractional-order design can also offer flexible parameters with better matching to experimental results.

To achieve optimal design, analysis of both magnitude and phase responses as well as sensitivity needs to be performed. Hence gradient-based optimization is introduced together with generalized fractional-order $RL_\beta C_\alpha$ circuits, as well as the inverse problems in filter design. Perfect matching has been observed between analytical solutions and PSpice simulation results [13]. The system response to typical 2nd order RLC circuits can be easily formulated via either KVL (Kirchhoff Voltage Law) or KCL (Kirchhoff Current Law). A series RLC circuit is shown in Fig. 1 while a parallel RLC circuit is shown in Fig. 2. When $t \geq 0$, series RLC circuit (Fig. 1) is formulated as the 2nd differential equation (1) via KVL.

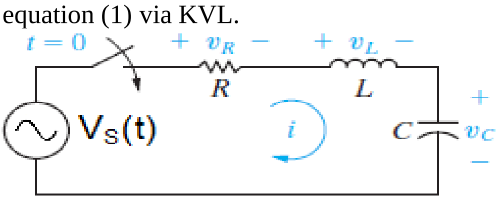

Fig. 1. Series 2nd order RLC circuit

$$\frac{d^2u_C(t)}{dt^2} + \frac{R}{L}\frac{du_C(t)}{dt} + \frac{1}{LC}u_C(t) = \frac{V_S(t)}{LC} \tag{1}$$

where $i(t) = C\frac{du_C(t)}{dt}$ and $v_L(t) = L\frac{di(t)}{dt} = LC\frac{d^2u_C(t)}{dt^2}$

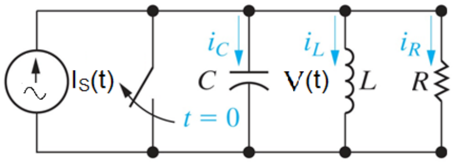

Fig. 2. Parallel 2nd order RLC circuit

Similarly when $t \geq 0$, parallel RLC Circuit (Fig. 2) can be formulated as another 2nd differential equation (2) via KCL.

$$\frac{d^2i_L(t)}{dt^2} + \frac{1}{RC}\frac{di_L(t)}{dt} + \frac{1}{LC}i_L(t) = \frac{I_S(t)}{LC} \tag{2}$$

where $v(t) = L\frac{di_L(t)}{dt}$ and $i_C(t) = C\frac{dv(t)}{dt} = LC\frac{d^2i_L(t)}{dt^2}$

In this preliminary research, the fractional order $RL_\beta C_\alpha$ circuits will be analyzed thoroughly, where the 2nd order RLC circuits will serve as a reference in order to compare characteristics depicted across various under-damped, critically-damped, and over-damped cases. Classical fractional Riemann-Liouville derivatives will be applied to the generalized equations of the series and parallel $RL_\beta C_\alpha$ fractional order circuits.

2 Mathematical models of fractional order circuits

The fractional order $RL_\beta C_\alpha$ circuits are formulated as the fractional order differential equations in this session, covering both the series $RL_\beta C_\alpha$ circuit and parallel $RL_\beta C_\alpha$ circuit. In the fractional order circuit, pseudo inductance (L_β) and pseudo capacitance (C_α) are introduced to substitute L and C in the 2nd order RLC circuits. When $t \geq 0$, the series fractional order $RL_\beta C_\alpha$ circuit could be reformulated via KVL as an $(\alpha+\beta)^{th}$ order differential equation.

$$\frac{d^{\alpha+\beta}u_C(t)}{dt^{\alpha+\beta}} + \frac{R}{L_\beta}\frac{d^\alpha u_C(t)}{dt^\alpha} + \frac{1}{L_\beta C_\alpha}u_C(t) = \frac{V_S(t)}{L_\beta C_\alpha} \tag{3}$$

where $i(t) = C_\alpha \frac{d^\alpha u_C(t)}{dt^\alpha}$ and $v_L(t) = L_\beta \frac{d^\beta i(t)}{dt^\beta}$.

The corresponding frequency domain transfer function from the classical control theory and the time domain state space models (state equation, output equation) from the modern control theory are expressed as (4)-(6), respectively.

$$\frac{U_C(s)}{V_S(s)} = \frac{1/L_\beta C_\alpha}{s^{\alpha+\beta} + (R/L_\beta)s^\alpha + (1/L_\beta C_\alpha)} \tag{4}$$

$$\begin{bmatrix} \frac{d^\alpha u_C(t)}{dt^\alpha} \\ \frac{d^\beta i(t)}{dt^\beta} \end{bmatrix} = \begin{bmatrix} 0 & \frac{1}{C_\alpha} \\ -\frac{1}{L_\beta} & -\frac{R}{L_\beta} \end{bmatrix} \begin{bmatrix} u_C(t) \\ i(t) \end{bmatrix} + \begin{bmatrix} 0 \\ \frac{1}{L_\beta} \end{bmatrix} V_S(t) \tag{5}$$

$$u_C(t) = \begin{bmatrix} 1 & 0 \end{bmatrix} \begin{bmatrix} u_C(t) \\ i(t) \end{bmatrix} \tag{6}$$

Meanwhile when $t \geq 0$, a parallel fractional order $RL_\beta C_\alpha$ circuit can be reformulated via KCL as another $(\alpha+\beta)^{th}$ order differential equation.

$$\frac{d^{\alpha+\beta}i_L(t)}{dt^{\alpha+\beta}} + \frac{1}{RC_\alpha}\frac{d^\beta i_L(t)}{dt^\beta} + \frac{1}{L_\beta C_\alpha}i_L(t) = \frac{I_S(t)}{L_\beta C_\alpha} \tag{7}$$

where $v(t) = L_\beta \frac{d^\beta i_L(t)}{dt^\beta}$ and $i_C(t) = C_\alpha \frac{d^\alpha v(t)}{dt^\alpha}$.

The corresponding frequency domain transfer function and the time domain state space models (state equation, output equation) are expressed as (8)-(10), respectively.

$$\frac{I_L(s)}{I_S(s)} = \frac{1/L_\beta C_\alpha}{s^{\alpha+\beta} + (1/RC_\alpha)s^\beta + (1/L_\beta C_\alpha)} \tag{8}$$

$$\begin{bmatrix} \frac{d^{\beta} i_L(t)}{dt^{\beta}} \\ \frac{d^{\alpha} v(t)}{dt^{\alpha}} \end{bmatrix} = \begin{bmatrix} 0 & \frac{1}{L_{\beta}} \\ -\frac{1}{C_{\alpha}} & -\frac{1}{RC_{\alpha}} \end{bmatrix} \begin{bmatrix} i_L(t) \\ v(t) \end{bmatrix} + \begin{bmatrix} 0 \\ \frac{1}{C_{\alpha}} \end{bmatrix} I_S(t) \tag{9}$$

$$i_L(t) = \begin{bmatrix} 1 & 0 \end{bmatrix} \begin{bmatrix} i_L(t) \\ v(t) \end{bmatrix} \tag{10}$$

From mathematical modeling points of view, there is almost no difference between (3) and (7). Thus without loss of generality, the factional order series $RL_{\beta}C_{\alpha}$ circuit is chosen for further analysis in this study, while those factional order parallel $RL_{\beta}C_{\alpha}$ circuits could generate identical results. Numerical simulations will include 3 separate cases of the underdamping, critical damping and over-damping, respectively.

3 Fractional order derivatives

Riemann-Liouville and Liouville–Caputo definitions are 2 typical forms of fractional derivatives. Being the fundamental one, the Riemann-Liouville definition is applied in this study which is simply formulated as (11), where m is an integer which satisfies $(m-1)<\alpha<m$. $\Gamma(.)$ represents the Euler's Gamma function that is defined as $\Gamma(n)=(n-1)!$ for an arbitrary positive integer n. D_R is the fractional derivative operator defined in (12). The real number fractional order is denoted as α.

$$D_R^{\alpha} f(t) = \begin{cases} \frac{1}{\Gamma(m-\alpha)} \frac{d^m}{dt^m} \int_0^t \frac{f(\tau)}{(t-\tau)^{\alpha+1-m}} d\tau \ (m-1 \le \alpha \le m) \\ \frac{d^m f(t)}{dt^m} \qquad (\alpha = m) \end{cases} \tag{11}$$

and

$$D_R^{\alpha} = \begin{cases} \frac{d^{\alpha}}{dt^{\alpha}} & (\alpha > 0) \\ 1 & (\alpha = 0) \\ \int_{\alpha}^{t} (d\tau)^{-\alpha} & (\alpha < 0) \end{cases} \tag{12}$$

The fractional derivative in (12) has an equivalent formulation, which serves as an alternative approach on a basis of finite differences and interpolation. It is also known as the Grünwald–Letnikov definition of fractional derivatives. It can be formulated as (13), where h represents the step size.

$$D_G^{\alpha} f(t) = \lim_{h \to 0} \frac{1}{h^{\alpha}} \sum_{m=0}^{(t-\alpha)/h} (-1)^m \frac{\Gamma(\alpha+1)}{m!\Gamma(\alpha-m+1)} f(t-mh) \tag{13}$$

4 Numerical simulations of DC series $RL_{\beta}C_{\alpha}$ circuits

In the numerical simulations, circuit parameters being selected are listed as below:

DC Voltage Source (V_S) = 5 Volt

Pseudo Inductance (L_{β}) = 2.0 Henry/sec$^{(1-\beta)}$

Pseudo Capacitance (C_{α}) = 0.5 Farad/sec$^{(1-\alpha)}$

In order to represent 3 cases of underdamping, critical damping and overdamping associated with the RLC natural response, the resistance R has been specified as 1.0, 4.0, and 10.0 Ohm, respectively.

The fractional orders of both capacitors ($0<\alpha<2$) and inductors ($0<\beta<2$) are selected as 0.25, 0.50, 0.75 1.00, 1.25, 1.50, 1.75, respectively. Some typical numerical simulation results are shown in Figs. 3-13 so as to make comparisons among various characteristic curves of the DC series $RL_\beta C_\alpha$ circuits.

From DC characteristics in Fig. 3 (critical damping), the fractional order ß of the series $RL_\beta C_\alpha$ circuit has larger impact on circuit characteristics than the fractional order α, which results in 3 distinctive characteristic curve sets significantly different from each other.

Within each of 3 sets though, the fractional order α leads to minor differences among 3 cases. In other words, major changes of characteristic curves arise from diverse fractional order ß while minor changes arise from diverse fractional order α for series $RL_\beta C_\alpha$ circuits (The role is opposite to parallel $RL_\beta C_\alpha$ circuits).

For α and ß in general, the big fractional order is corresponding to the large overshoot and short settling time. But if α and ß are too big, increasing oscillation will occur rather than sustained oscillation and decaying oscillation, the system turns out to be unstable.

The critical-damping only exists in the 2nd order series RLC circuit instead of any other fraction order case. The smallest pair of α and ß on the other hand, could produce the highest instantaneous input surge current (spike), which could damage the electronic devices.

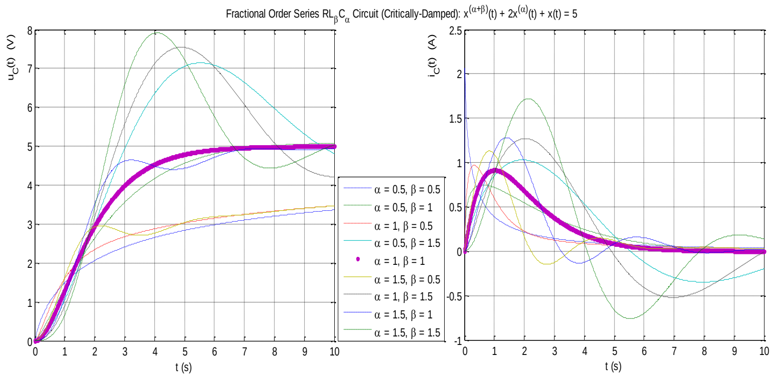

Fig. 3. $U_C(t)$ and i(t) of DC series $RL_\beta C_\alpha$ circuit (critical damping)

In Figs. 4-12, I-V characteristics of DC series $RL_\beta C_\alpha$ circuits are shown, covering all three cases of underdamping, critical-damping and overdamping with various combinations of the fractional order α and fractional order ß, where the 2nd order series RLC circuit (purple curve) acts as the reference (scale varies remarkably across various cases). In Figs. 4-6, under-damped I-V characteristics (DC) are shown. The largest fractional orders pair α and ß (e.g. α=ß=1.75) will lead to enormous levels of overshoots in the voltage and current. For smallest fractional orders pair α and ß (e.g. α=ß=0.25), the highest input surge current is generated instead.

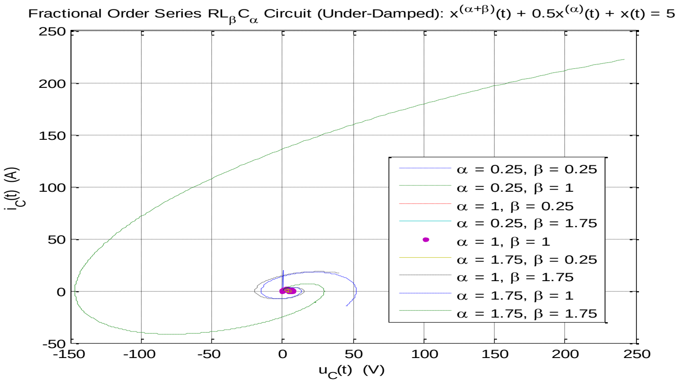

Fig. 4. I-V characteristics of DC $RL_\beta C_\alpha$ circuit (case 1)

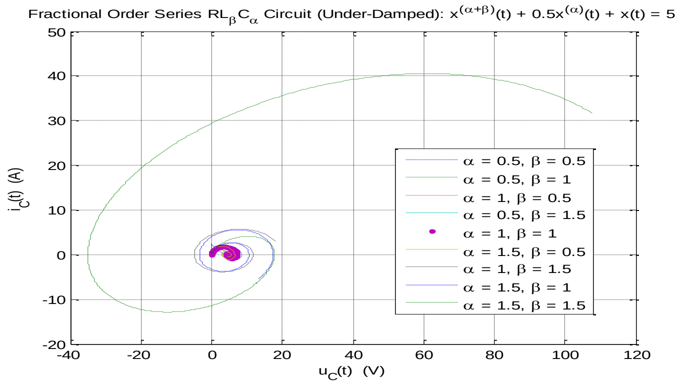

Fig. 5. I-V characteristics of DC $RL_\beta C_\alpha$ circuit (case 2)

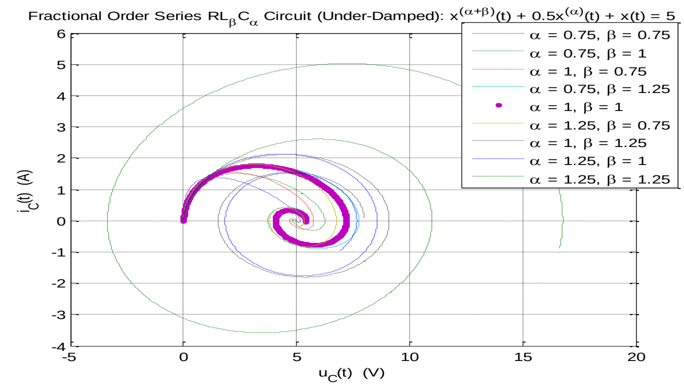

Fig. 6. I-V characteristics of DC $RL_\beta C_\alpha$ circuit (case 3)

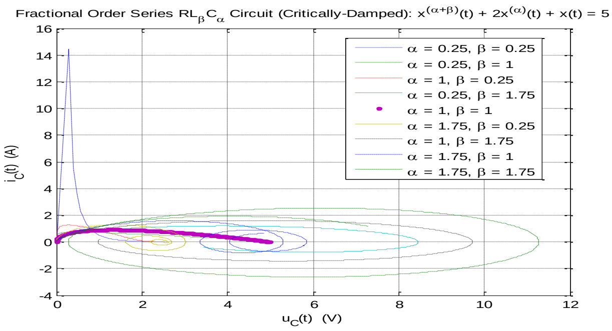

Fig. 7. I-V characteristics of DC $RL_{\beta}C_{\alpha}$ circuit (case 4)

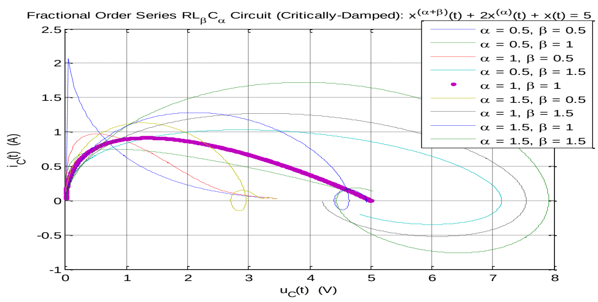

Fig. 8. I-V characteristics of DC $RL_{\beta}C_{\alpha}$ circuit (case 5)

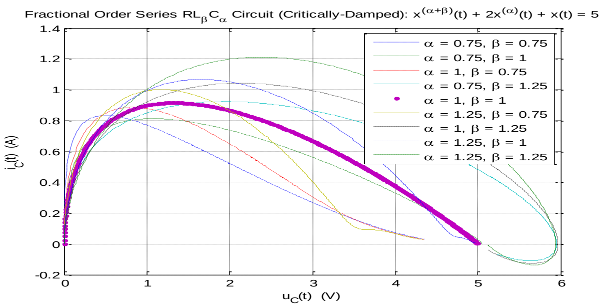

Fig. 9. I-V characteristics of DC $RL_{\beta}C_{\alpha}$ circuit (case 6)

In Figs. 7-9, critically-damped I-V characteristics (DC) of series $RL_{\beta}C_{\alpha}$ circuits are shown. Although the critically-damped response and over-damped response of the 2nd order RLC circuit generally exhibit no overshoot or oscillation, overshoot could occur however in the critically-damped response when the large fractional order pair α and ß (e.g. α=ß=1.75) are selected. On the other hand, small fractional order pair α and ß (e.g. α=ß=0.25) instead will result in much larger level of input surge current than the underdamped case. The smaller the fractional order is, the larger the input surge current is. In fact the abrupt instantaneous current spike is relevant to the step response of reactive elements. In Figs. 10-12, over-damped I-V characteristics (DC) of series

$RL_\beta C_\alpha$ circuits are shown. Unlike the 2nd order RLC circuit case, overshoot could even possibly occur in the over-damped response of series $RL_\beta C_\alpha$ circuits when the large fractional order pair (e.g. α=ß=1.75) are applied, while the settling time would be reduced significantly. Still the small fractional order pair α and ß (e.g. α=ß=0.25) could give rise to a huge level of the input surge current, but less than the critically-damped response of series $RL_\beta C_\alpha$ circuits. The less fractional orders are, the higher the initial surge current is.

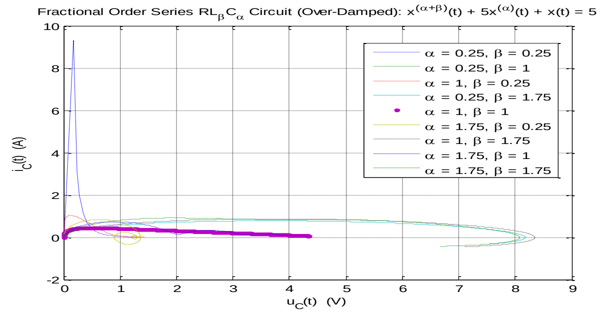

Fig. 10. I-V characteristics of DC $RL_\beta C_\alpha$ circuit (case 7)

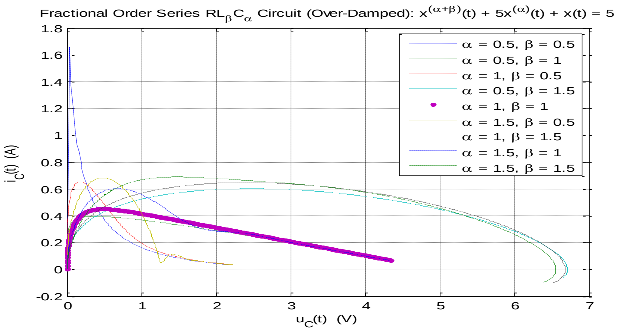

Fig. 11. I-V characteristics of DC $RL_\beta C_\alpha$ circuit (case 8)

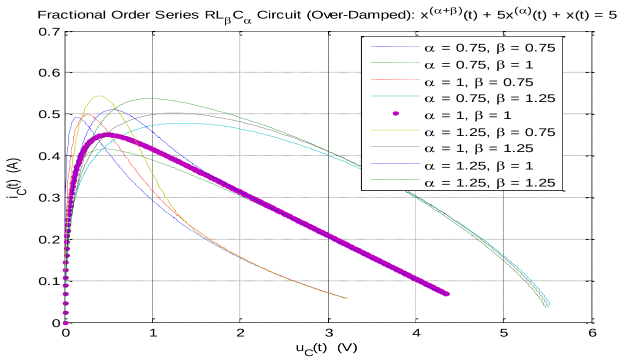

Fig. 12. I-V characteristics of DC $RL_\beta C_\alpha$ circuit (case 9)

5 Numerical simulations of AC series $RL_\beta C_\alpha$ circuits

For 2nd order AC series RLC circuits in (1-2), there are 2 dominating parameters to manifest the behaviors: the resonant frequency and the damping ratio. The resonant frequency is computed as (14) while the damping ratios ζ_S and ζ_P can be computed as (15), corresponding to the 2nd order series and parallel RLC circuits respectively. The quality factor (Q-factor) acts as a frequency-to-bandwidth (full width at half maximum) ratio of the resonator, which is relevant to the damping ratio and expressed as (16). Generalized fractional order reactive elements are expressed as (17) and (18) instead, representing the pseudo inductance and pseudo capacitance.

$$\omega_r = 1/\sqrt{LC}\ (rad/sec)\ \ and\ \ f_r = 1/(2\pi\sqrt{LC})\ (Hz) \tag{14}$$

$$\zeta_S = \frac{R}{2}\sqrt{\frac{C}{L}}\ \ and\ \ \zeta_P = \frac{1}{2R}\sqrt{\frac{L}{C}} \tag{15}$$

$$Q = \frac{1}{2\zeta} = \frac{\omega_r}{\Delta\omega} \tag{16}$$

$$L_\beta = \omega^{1-\beta} L/sin(\frac{\beta\pi}{2})\ \ and\ \ L = \omega^{\beta-1} L_\beta sin(\frac{\beta\pi}{2}) \tag{17}$$

$$C_\alpha = \omega^{1-\alpha} C sin(\frac{\alpha\pi}{2})\ \ and\ \ C = \omega^{\alpha-1} C_\alpha/sin(\frac{\alpha\pi}{2}) \tag{18}$$

At resonance, we have (19) being satisfied. The resonant frequency of fractional order $RL_\beta C_\alpha$ circuits can thus be directly computed as (20).

$$LC\omega^2 = \omega_{FO}^{\alpha+\beta} L_\beta C_\alpha sin(\frac{\beta\pi}{2})/sin(\frac{\alpha\pi}{2}) = 1 \tag{19}$$

$$\omega_{FO} = \sqrt[(\alpha+\beta)]{\frac{sin(\alpha\pi/2)}{L_\beta C_\alpha sin(\beta\pi/2)}}\ \ and\ \ f_{FO} = \frac{\omega_{FO}}{2\pi} \tag{20}$$

In the numerical simulations, circuit parameters being selected are similar to those in the DC fractional order series $RL_\beta C_\alpha$ circuits, except for the AC power source, where US standard AC voltage is adopted instead: $V_S(t) = 120\sqrt{2}cos(120\pi t)$Volt. Again to represent 3 cases of underdamping, critical-damping and overdamping of the natural response, the resistance R has been specified as 1.0, 4.0, and 10.0 Ohm, respectively. When either α=β or (α+β)=2 holds, the fractional order $RL_\beta C_\alpha$ circuit has exactly the same resonant frequency as that of the typical 2nd order RLC circuit, where the resonant angular frequency 1.0 rad/sec acts as a reference in several cases above. The damping ratio however is defined for the 2nd order circuit exclusively. As for potential stability control in the worst case scenario, the circuit parameters chosen in simulations match the resonance condition, which is related to maximal amplitudes of the AC voltage and AC current to be controlled. Fractional orders for capacitors ($0<\alpha<2$) and inductors ($0<\beta<2$) are selected as 0.25, 0.50, 0.75 1.00, 1.25, 1.50 and 1.75, respectively. Typical numerical simulation results are shown in Figs. 13-22, to make comparisons among various characteristic curves of the AC series $RL_\beta C_\alpha$ circuits. From AC characteristics in Fig. 13 (critical damping), the fractional order ß of series $RL_\beta C_\alpha$ circuits has larger impact on circuit characteristics than fractional order α, which leads to 3 distinctive characteristic curve sets significantly different from each other. Within each of 3 sets though, the fractional order α leads to minor differences among 3 cases. Major changes of characteristic curves arise from diverse fractional order ß while minor changes arise from diverse fractional order α (The role is opposite to parallel $RL_\beta C_\alpha$ circuits). For both α and ß, in general, the smaller the fractional order is, the earlier the time advance is and the larger the I-V characteristic curve magnitude is (vice versa). Fractional orders α and ß will affect both the amplitude and time shifting (delay or advance) in characteristic curves, covering the magnitude response and phase response.

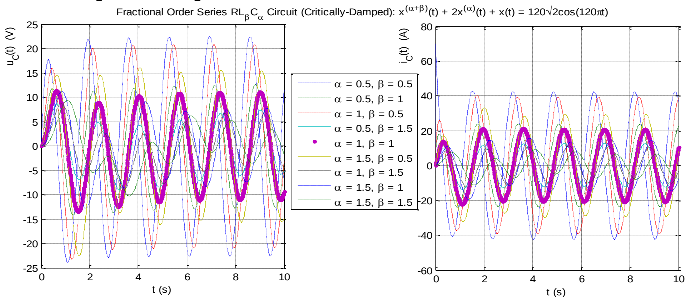

Fig. 13. $U_C(t)$ and i(t) of AC series $RL_\beta C_\alpha$ circuit (critical damping)

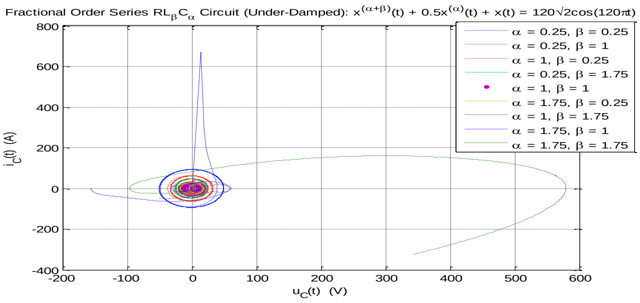

Fig. 14. I-V characteristics of AC $RL_\beta C_\alpha$ circuit (case 1)

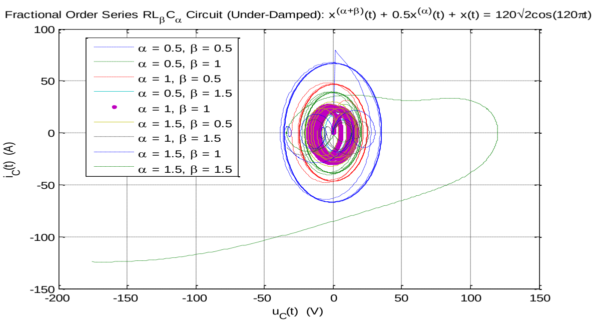

Fig. 15. I-V characteristics of AC $RL_\beta C_\alpha$ circuit (case 2)

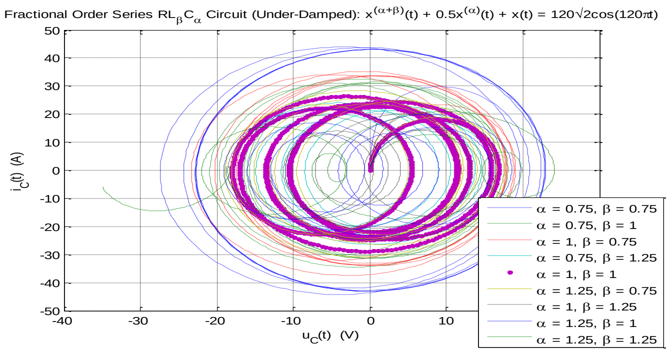

Fig. 16. I-V characteristics of AC $RL_{\beta}C_{\alpha}$ circuit (case 3)

In Figs. 14-22, I-V characteristics of AC series $RL_{\beta}C_{\alpha}$ circuits are shown, including all three cases of under-damping, critical-damping and over-damping, where the 2nd order AC series RLC circuit acts as a reference (scale varies remarkably).

In Figs. 14-16, under-damped I-V characteristics (AC) are shown. The largest fractional orders pair α and ß (e.g. α = ß = 1.75) could also generate increasing oscillation for AC series $RL_{\beta}C_{\alpha}$ circuits. Smallest fractional orders pair α and ß (e.g. α=ß=0.25) will generate highest level of instantaneous input surge current in the starting cycle. The characteristic curves are significantly different from the 2nd order RLC circuits.

In Figs. 17-19, critically-damped I-V characteristics (AC) are shown. The smallest fractional order pair α and ß (e.g. α = ß = 0.25) will generate an exceptional level of instantaneous input surge current in the starting cycle. The smaller the fractional order pair is, the larger the surge current is. The I-V characteristic curves will circle around the equilibrium after initial cycles, showing behaviors of sustained oscillation.

In Figs. 20-22, over-damped I-V characteristics (AC) are shown. Still the smallest fractional order pair α and ß (e.g. α=ß=0.25) will give rise to extra level of instantaneous input surge current in the starting cycle, but its impact is less than the critical-damping case. The smaller the fractional order pair is, the larger the surge current is. The I-V characteristic curves circle around the equilibrium after initial cycles.

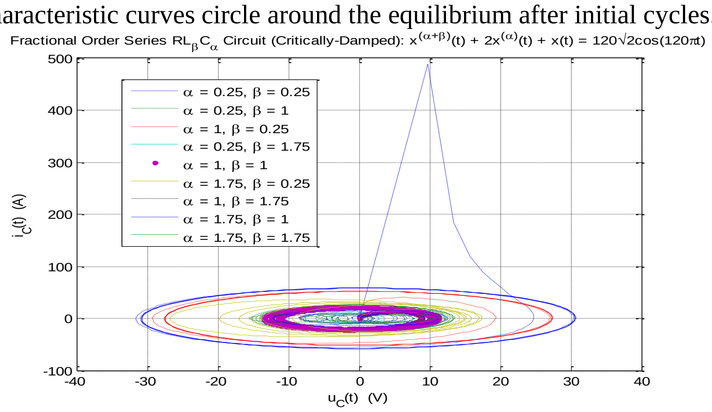

Fig. 17. I-V characteristics of AC $RL_{\beta}C_{\alpha}$ circuit (case 4)

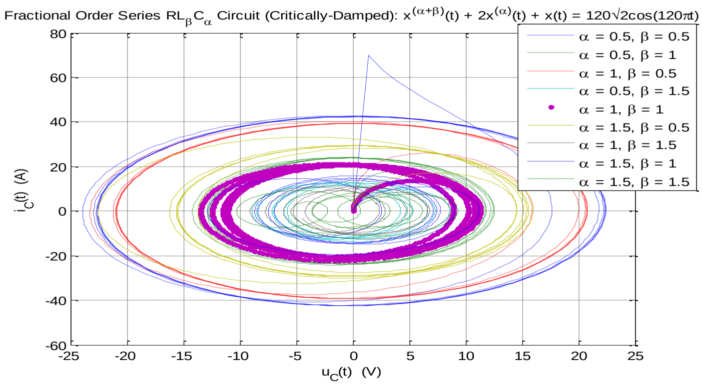

Fig. 18. I-V characteristics of AC $RL_\beta C_\alpha$ circuit (case 5)

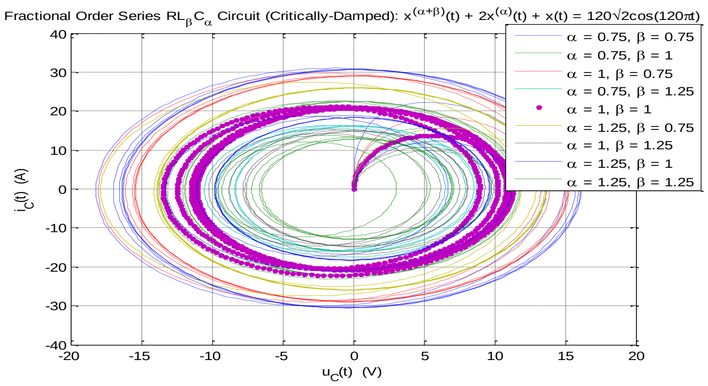

Fig. 19. I-V characteristics of AC $RL_\beta C_\alpha$ circuit (case 6)

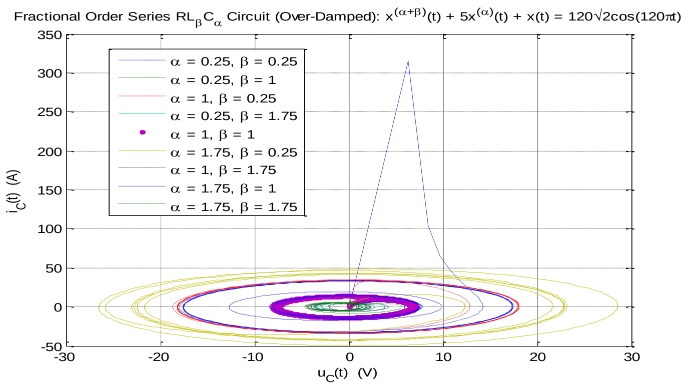

Fig. 20. I-V characteristics of AC $RL_\beta C_\alpha$ circuit (case 7)

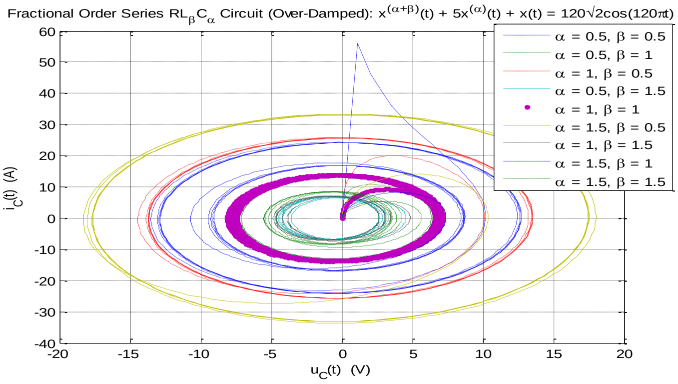

Fig. 21. I-V characteristics of AC $RL_\beta C_\alpha$ circuit (case 8)

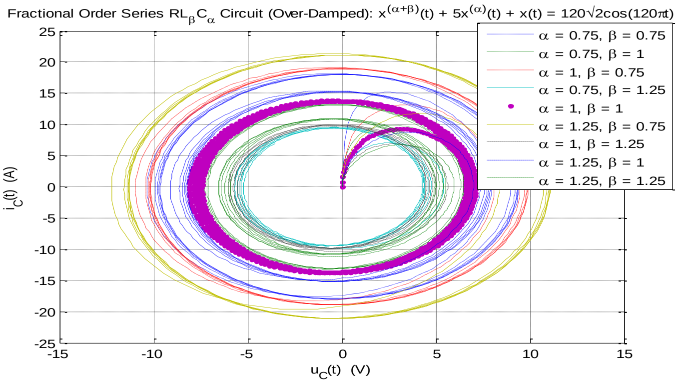

Fig. 22. I-V characteristics of AC $RL_\beta C_\alpha$ circuit (case 9)

6 Conclusion

The fractional order $RL_\beta C_\alpha$ circuit has been analyzed in this preliminary study. It can deliver more flexibility for potential stability control and performance enhancement than the 2nd order RLC circuits. The series fractional order $RL_\beta C_\alpha$ circuit is applied as the example for characteristic analysis where the fractional Riemann-Liouville derivatives are applied. Various DC and AC circuit cases with different fractional order pair α and β are taken into account for comparison purposes. The stability issue has been the focus of the DC fractional order $RL_\beta C_\alpha$ circuit through the step response analysis. The magnitude transient response (magnitude) and time shifting (phase) are both emphasized in AC fractional order $RL_\beta C_\alpha$ circuit analysis at the resonant frequency. I-V characteristics are presented on all three cases of underdamping, critical-damping and overdamping via numerical simulations. It shows that the fractional order β has greater impact than fractional order α on characteristics of series fractional order $RL_\beta C_\alpha$ circuits in general, no matter if the DC or AC circuit is applied. The large pair of the fractional order α and β takes the leading role in system stability, while the small pair of the fractional order α and β has negative influence in the instantaneous input surge current at the starting stage. This research work has provided the useful insights into the potential stability problems in numerous engineering applications such as dynamic control, robotics, mechatronics and communication.

References

1. Gutiérrez R., Rosário J., and Tenreiro J.: Fractional order calculus: basic concepts and engineering applications. Mathematical Problems in Engineering Journal, pp. 1-19 (2010)
2. Ye Z.: "Modeling, identification, design and implementation of nonlinear automotive idle speed control systems - an overview", IEEE Transactions on Systems, Man and Cybernetics, Part C: Applications and Reviews, Vol. 37, No. 6, pp. 1137-1151 (2007)
3. Ye Z., Mohamadian H., and Yin H.: Impact of fractional orders on characteristics of chaotic dynamical systems. International Journal of Electrical, Electronics and Data Communication, Vol. 5, Issue 2, pp. 72-77 (2017)
4. Tsirimokou G., Psychalinos C., Elwakil A., and Salama K: Electronically tunable fully integrated fractional-order resonator. IEEE Transactions on Circuits and Systems II: Express Briefs, Vol. 65, No. 2, pp. 166-170 (2018)
5. Ye Z., Yin H., and Meng A.: Comparative studies of DC motor FOPID control with optimal state estimation using kalman filter. In Proceedings of International Conference on Power Electronics and Their Applications, September 25-27, Elazig, Turkey (2019)
6. Ye Z., and Mohamadian H.: Application of modern control theory on performance analysis of generalized notch filters. In Proceedings of International Conference on Modern Circuits and Systems Technologies, May 12-14, 2016, Thessaloniki, Greece (2016)
7. Ye Z., and Mohamadian H.: Comparative study of generalized electrical and optical notch filters via classical control theory. In Proceedings of International Conference on Modern Circuits and Systems Technologies, May 12-14, Thessaloniki, Greece (2016)
8. Zhang G., Ou Z., and Qu L.: A fractional-order element based approach to wireless power transmission for frequency reduction and output power quality improvement. MDPI Journal of Electronics, Vol. 8, pp. 14 (2019)
9. Dimeas I., Tsirimokou G., Psychalinos C. and Elwakil A.: Realization of fractional-order capacitor and inductor emulators using current feedback operational amplifiers. In Proceedings of International Symposium on Nonlinear Theory and its Applications, December 1-4, 2015, Kowloon, Hong Kong, China, pp. 237-240 (2015)
10. Gomez F., Rosales J., and Guia M.: RLC electrical circuit of non-integer order. Central European Journal of Physics, Vol. 11, No. 10, pp. 1361-1365 (2013)
11. Stankiewicz A.: Fractional order RLC circuits. In Proceedings of 2017 International Conference on Electromagnetic Devices and Processes in Environment Protection with Seminar Applications of Superconductors, pp. 4, December 3-6, 2017, Lublin, Poland (2017)
12. Alsaedi A., Nieto J., and Venktesh V.: Fractional electrical circuits. Advances in Mechanical Engineering Journal, Vol. 7 (12), pp. 1–7 (2015)
13. Walczak J., Jakubowska A.: Resonance in series fractional order $RL_{\beta}C_{\alpha}$ circuit. Przegląd Elektrotechniczny, R. 90, No. 4, pp. 210-213 (2014)